

PC-based spinning rotor gage controller

J. P. Looney, F. G. Long, D. F. Browning, and C. R. Tilford
Thermophysics Division, National Institute of Standards and Technology, Gaithersburg, Maryland 20899

(Received 8 April 1994; accepted for publication 10 June 1994)

The spinning rotor gage (SRG) is a molecular drag vacuum gage. Commercial versions are available that operate between about 10^{-4} and 1 Pa. In this paper we describe the design, and present performance data for a new SRG controller that uses a plug-in peripheral board and a personal computer (PC) to perform all control, signal processing, and data analysis functions. This controller offers several advantages over those presently available, including the simultaneous operation of multiple SRGs (at least four SRGs with a single PC), complete software control of all operating parameters, and significantly improved low-pressure performance.

I. INTRODUCTION

The idea of using the molecular drag on a moving body to measure the density or pressure of low-pressure gases dates back to the last century. Early implementations of this idea were limited by the difficulties of measuring small angular deviations, or the oscillatory amplitude decay, of bodies suspended from torsion fibers. Beams and co-workers¹ overcame these difficulties by substituting a magnetic suspension for the torsion fiber, allowing the pressure to be determined from the rate of decay of the rotation of a freely rotating ball. Practical development of Beam's spinning rotor gage (SRG) was advanced at the Kernforschungsanlage (KFA)—Jülich with the development of an automated magnetic suspension system, and the use of an inductively detected signal to time the rotation of the suspended ball.² The commercial introduction of the SRG followed a little over ten years ago.

The introduction of the commercial SRG was a significant advance in vacuum measurements as it offers several advantages compared to conventional vacuum gages. It is more sensitive than mechanical-deflection gages and can be used throughout the high-vacuum range. It is more stable than ionization or thermal conductivity gages—its calibration typically changes by no more than 1%–2% over several years time.³ It does not perturb the vacuum environment with a hot cathode (filament) or high-voltage discharge, and it is compatible with a wide variety of gases, including corrosive gases. These characteristics have led to the widespread use of the SRG as a reference standard for the calibration of other vacuum gages between 10^{-4} and 10^{-1} Pa (10^{-6} and 10^{-3} Torr), and offer potential for monitoring chemically active process gases. The SRG can also be used at pressures well above this range with the addition of a correction for gas-viscosity effects.

However, the commercial SRG does suffer some limitations, particularly in the electronic control unit (controller). Its operation is highly automated and controlled by a microprocessor and hard-wired logic, which does not allow user intervention or modification of several important functions. The useful range of the gage is limited at the low end primarily by the measuring time, which is restricted by the hard-wired logic to a maximum of 30 s—corresponding to an imprecision (standard deviation) in the measured pressure of about 10^{-6} Pa. At the other extreme, measurement of pres-

ures above 10^{-1} Pa require a viscosity correction, and the corrections incorporated into the current commercial controllers have significant errors for pressures above 10 Pa,⁴ which requires post processing to correct. Not incidentally, the cost of the controller is about \$10 000.

These problems prompted the NIST Vacuum Group to undertake the development of an SRG controller that would permit user control of all parameters, including the choice of automatic operation or manual override of all functions, updated control and data analysis software as needed, and longer measurement times. This effort has resulted in a controller with all of the electronics on a single personal computer (PC) plug-in board, and all of the data processing and control functions lodged in user-accessible PC software. Measurement times are effectively unlimited, offering the potential for an order of magnitude extension of the range to lower pressures. This system has the additional advantage that at least four separate control boards and SRGs can be operated simultaneously by a single PC. This controller is compatible with the other commercial SRG components and is, in effect, a plug-in replacement for the commercial control units. This paper describes the important elements of the new controller, particularly the signal processing circuitry and an essential data processing algorithm, and presents low-pressure performance data.

II. BASIC DESCRIPTION OF THE SRG

The SRG has three main components: (1) The sensor or rotor; a magnetic steel bearing ball located in a thimble, a thin-walled extension of the vacuum system. (2) The suspension head; located outside the thimble, it contains permanent and electromagnets to suspend the ball, suspension coils to sense and stabilize the position of the suspended ball, inductive-drive coils to spin the ball to its operating frequency range, and pickup coils to sense the rotation of the ball. (3) The electronic control unit (controller); which controls all operating functions, amplifies the pickup signal from the rotating ball, and processes the data from the signal to obtain the pressure. When the power is turned on, the current generation of commercial controllers automatically suspends and stabilizes the ball and powers the inductive-drive coils to spin the ball to a preselected frequency range, typically 405–415 Hz. The drive power is turned off and the ball allowed to

coast. The magnetic moment(s) of the rotating ball induces a signal in the pickup coils that is used to monitor the rotation rate. This pickup signal is processed to calculate the rotational decay rate, and corrections are applied to convert this to an equivalent pressure.

From kinetic theory it can be shown that collisions with gas molecules cause the ball's rotation frequency to exponentially decrease, or the rotation period τ to exponentially increase with time t ,

$$\tau = \tau_0 \exp^{KPt}, \quad (1)$$

where P is the pressure, and K is a calibration constant; given by $K = \pi \rho a \bar{c} / 10 \sigma_{\text{eff}}$ where ρ is the density of the ball, a is its radius, \bar{c} is the mean gas molecular speed (which depends on the gas temperature and molecular weight), and σ_{eff} is the effective tangential-momentum accommodation coefficient.³ The effective accommodation coefficient accounts for the surface roughness of the ball and molecular scattering characteristics; for "smooth" balls σ_{eff} is typically between 0.95 and 1.07 (more accurate determination requires calibration against a vacuum standard).

From Eq. (1) and its time derivative one obtains

$$P = \frac{1}{K} \left(\frac{\dot{\tau}}{\tau} \right). \quad (2)$$

Thus the logarithmic time derivative of the rotor period, $\dot{\tau}/\tau$, is the essential factor that must be determined.

Determination of the time derivative is not trivial. For typical SRG operating conditions it is very small; a nitrogen pressure of 10^{-4} Pa causes the period to increase at a fractional rate of about $10^{-7}/\text{s}$, corresponding to a time constant of three years. Further, the available information, the signal from the pickup coils, leaves much to be desired; the typical signal induced by the rotating magnetic moment(s) has a magnitude of 10–100 μV , but is accompanied by as much as a millivolt of noise from various sources, including power line, vibration-induced, and thermal or Johnson noise from the pickup coils. Determination of the time derivative from this signal requires careful attention to both signal processing and data analysis.

As described more fully in Sec. IV A, the pickup signal is amplified, filtered, and converted to a square wave—the zero crossings of the square wave define the rotation period. The times of successive zero crossings are measured with respect to a clock or reference oscillator and combined to determine the time derivative. However, even with careful amplification and filtering, the zero-crossing times still have a significant phase noise or time jitter, typically a few microseconds. The effects of the time jitter can be reduced significantly by statistically combining a number of zero-crossing times, with the results strongly dependent on the number of zero crossings or the measuring time. With the data processing algorithm described in Sec. III and a measurement time of 100 s, a rotation period of a few milliseconds can be determined with an imprecision of a few picoseconds, in spite of the microsecond time jitter. Since the success of the SRG depends on the ability to determine the logarithmic time derivative precisely, the data processing algorithm will be derived in some detail.

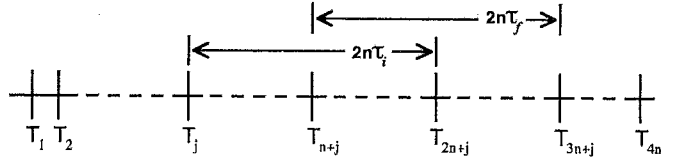
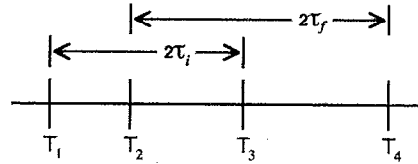


FIG. 1. Schematic illustration of two different ways to obtain the change of period from averages over multiple periods. The top line (with greatly exaggerated period differences) illustrates the simplest case. The bottom line illustrates one of the n independent averages that can be obtained from $4n$ measured zero crossings.

III. LOGARITHMIC TIME DERIVATIVE ALGORITHM

A small body of literature has been developed on the techniques of measuring the frequency of noisy signals. For example, Snyder⁵ presents explicit algorithms and implementation techniques for a frequency meter that reduces the effects of phase noise. Similar approaches for determining the time derivative of the frequency (or period) are discussed by Fremerey.⁶ Basically, for both the frequency and its derivative, it is necessary to average over multiple rotation periods, with the best results obtained when all of the data (zero crossings) in a measurement interval are statistically combined.

The basic approach to deriving the time-derivative algorithms used in SRGs starts with the recognition that the time derivative is almost constant during a typical measurement time t . Therefore, Eq. (1) can be approximated as

$$\tau = \tau_0 [1 + KPt + \frac{1}{2}(KPt)^2 + \dots]. \quad (3)$$

For typical SRG operating conditions $10^{-6} < KPt < 10^{-4}$, and it is necessary to retain only the linear term in Eq. (3). With this linear approximation we can write

$$\frac{\dot{\tau}}{\tau} = \frac{\tau_f - \tau_i}{\Delta t \langle \tau \rangle}, \quad (4)$$

where τ_f and τ_i are final and initial rotation periods, separated by a time interval Δt , and $\langle \tau \rangle$ is the period averaged over this same interval. The rotational periods can be determined using the times of either the positive-going or the negative-going zero crossing to mark the beginning and end of successive rotation periods.

Equation (4) can be implemented with a minimum of two periods or three zero crossing. However, starting with four zero crossing results in algorithms that give equal statistical weight to all of the data and smaller imprecisions.

Designating the times of the i th zero crossing as T_i , we can use the times of four zero crossings and average over groups of two periods, as illustrated at the top of Fig. 1, to determine

$$\frac{\dot{\tau}}{\tau} = \frac{1/2(T_4 - T_2) - 1/2(T_3 - T_1)}{[1/2(T_4 + T_2) - 1/2(T_3 + T_1)]1/2[1/2(T_4 - T_2) + 1/2(T_3 - T_1)]} \quad (5)$$

Within the linear approximation, the two terms in the denominator, the time interval and the average period, are equal, so Eq. (5) can be rewritten to give

$$\frac{\dot{\tau}}{\tau} = \frac{8(T_1 - T_2 - T_3 + T_4)}{(-T_1 - T_2 + T_3 + T_4)^2} \quad (6)$$

While illustrative of the general approach, Eq. (6) does not achieve adequate imprecision for use with an SRG. As a first improvement, the interval over which the terms of Eq. (4) are averaged can be increased from 2 periods to $2n$ periods, with n an integer. For example, if $4n$ zero crossings are measured, as illustrated in Fig. 1, the change in period can be obtained as, $\tau_f - \tau_i = (T_{3n+j} - T_{n+j})/2n - (T_{2n+j} - T_j)/2n$, where j is any integer between 1 and n . Calculating similar averages for the other terms in Eq. (4), and noting that the time interval Δt is now n times the average period, we obtain the analog of Eq. (6);

$$\frac{\dot{\tau}}{\tau} = \frac{8[T_j - T_{n+j} - T_{2n+j} + T_{3n+j}]}{[-T_j - T_{n+j} + T_{2n+j} + T_{3n+j}]^2} \quad (7)$$

The imprecision of $\dot{\tau}/\tau$ determined with Eq. (7) is a factor of n better than that derived from Eq. (6).

A further improvement is possible since the $4n$ zero-crossing times allow n independent determinations of each of the terms in Eq. (4). To within the linear approximation, each of these values is equivalent, apart from statistical variation. Therefore, we can average these n values to obtain, for example,

$$\tau_f - \tau_i = \frac{1}{n} \sum_{j=1}^n \left(\frac{T_{3n+j} - T_{n+j}}{2n} - \frac{T_{2n+j} - T_j}{2n} \right) \quad (8)$$

Computing the same type of average value for each of the terms in Eq. (4), and rearranging as in Eqs. (6) and (7), we obtain

$$\frac{\dot{\tau}}{\tau} = \frac{8n(\sum_{j=1}^n T_j - \sum_{j=n+1}^{2n} T_j - \sum_{j=2n+1}^{3n} T_j + \sum_{j=3n+1}^{4n} T_j)}{(-\sum_{j=1}^n T_j - \sum_{j=n+1}^{2n} T_j + \sum_{j=2n+1}^{3n} T_j + \sum_{j=3n+1}^{4n} T_j)^2} \quad (9)$$

Equation (9) is straightforward to implement; once having established a measurement time and the equivalent value of n , the four sums required for the numerator and denominator are easily accumulated, either in hard wired up-down or gated counters, or in software. Software accumulation has the advantage of no effective limit to the value of n . Each measured zero-crossing time appears with equal weight, and as will be shown below, the imprecision of $\dot{\tau}/\tau$ determined with Eq. (9) decreases as $n^{-2.5}$.

the change in the period, e.g., $\tau_f - \tau_i = (T_4 - T_2)/2 - (T_3 - T_1)/2$. Using this same type of average for the other terms in Eq. (4), we obtain

So far, the analysis has used only half the available data—either the negative-going or the positive-going zero crossing. If the pickup signal is completely symmetric, e.g., a sine wave with zero offset, all the zero crossings can be used and the imprecision for a given measurement time reduced by $\sqrt{2}$. However, dc offsets within the signal amplifier can cause an asymmetry in the final square wave so that successive zero crossings are not evenly spaced, i.e., the signal half-periods will differ. If both zero crossings are used, and n is odd, this will cause the average time interval value in Eq. (4) to depend on whether the measurement starts with a positive-going or negative-going zero crossing—this could cause a significant error for small values of n . This error can be completely eliminated if n is selected to be even.

Note that the bracketed sum in the denominator of Eq. (9) is $4n^2$ times the average period, so that, using every other zero crossing, the period or frequency can be determined with a small imprecision from

$$\tau = \frac{1}{4n^2} \left(-\sum_{j=1}^{2n} T_j + \sum_{j=2n+1}^{4n} T_j \right) \quad (10)$$

(multiply by 2 if both negative-going and positive-going zero-crossing times are used). This is effectively the same as the algorithm presented by Snyder.⁵

A. Imprecision analysis

Because the low-pressure operating limit of the SRG is determined in large part by the imprecision of $\dot{\tau}/\tau$, we derive the imprecision of the value obtained from Eq. (9). Using standard analysis of variance techniques (the variance of a quantity is the square of its standard deviation), noting that Eq. (9) can be written as $\dot{\tau}/\tau = 8nA/B$, and designating the variance of x as $S(x)$, we have

$$S(\dot{\tau}/\tau) = \frac{64n^2}{B^4} S(A) + \frac{256n^2 A^2}{B^5} S(B) \quad (11)$$

Since A and B are each sums of $4n$ independent time measurements, the variances of A and B are $S(A) = S(B) = 4nS(T)$, where $S(T)$ is the square of the standard deviation of the measured times of the zero crossings.

Keeping in mind that $B = 4n^2\tau$, we have

$$S(\dot{\tau}/\tau) = \frac{S(T)}{n^5 \tau^4} (1 + n^2 \dot{\tau}^2) \quad (12)$$

However, at a pressure of 1 Pa $\dot{\tau}$ is about 10^{-3} and n is typically no larger than 100. As the pressure decreases, $\dot{\tau}$ decreases faster than n increases. Thus, for typical SRG op-

erating conditions the last term of Eq. (12) is much less than 1 and can be neglected. This confirms the intuitive observation that the dominant source of uncertainty is the determination of the small change in period, while the average period and the measurement interval contribute very little to the uncertainty. Therefore, to a very good approximation, the standard deviation or imprecision of the logarithmic time derivative, due to noise in the pickup signal, is

$$\sigma(\dot{\tau}/\tau) = \frac{\sigma(T)}{n^{5/2} \tau^2}, \quad (13)$$

where $\sigma(T)$ is the standard deviation of the measured times. Alternatively, if Δt is the measurement interval, and f is the operating frequency.

$$\sigma(\dot{\tau}/\tau) = \frac{32\sigma(T)}{\sqrt{f}(\Delta t)^{5/2}}. \quad (14)$$

Equations (13) and (14) illustrate the importance of long measuring times to low-pressure measurements. As will be shown in Sec. V, the experimental imprecisions of the measured pressures do decrease with the $5/2$ power of the measuring time (or the number of zero crossings), until they are limited by factors other than phase noise in the pickup signal. The increased measuring times possible with the new controller permit a reduction in the low-pressure limit of the SRG by one to two orders of magnitude.

In general, reference clock oscillator zero crossings are highly correlated (small random errors) and their contribution to the uncertainty of the time derivative is negligible. Further, for good-quality quartz oscillators, frequency drifts over typical measurement periods (up to a few minutes) are small enough that they do not contribute significant errors. However, all of the pickup signal zero-crossing times have a clock-quantization error between 0 and τ_{ref} , where τ_{ref} is the period of the reference oscillator. To within the random variations of the zero crossings, these quantization errors are correlated, further, they can be made small relative to the zero-crossing errors by using a high reference frequency, i.e., a small τ_{ref} .

IV. CIRCUITRY AND THE DECELERATION RATE MEASUREMENT

As shown in the last section, accurate values of the deceleration rate (DCR) of the rotor, and hence of the pressure, can be determined from measurements of $4n$ (where n is large) pickup signal zero-crossing times. The time of each zero crossing is determined by counting the number of reference clock cycles which elapse between zero crossings. The reference clock counts are accumulated in an on-board counter, and transferred to the PC after each zero crossing. The counter readings are added in software to a running sum to maintain a cumulative time scale. The sums needed for Eqs. (9) and (10) are also performed in PC software, rather than with hard-wired accumulators and logic circuits. Zero crossings occur roughly every millisecond or so, and thus the host computer needs to be sufficiently fast to respond to a data-ready flag, read the clock counts, add the clock counts to the appropriate sum in Eq. (9), and be ready to respond to

the next data-ready flag. With modern PCs this can easily be done for several SRG controller boards operating simultaneously.

The PC-based SRG controller consists of six circuits: (1) the suspension and vertical stabilization circuit, (2) the horizontal or lateral stabilization circuit, (3) the motor brake and drive circuit, (4) the signal amplification circuit, (5) the counter circuit, and (6) the computer-SRG controller board interface circuit. The suspension, lateral stabilization, and brake/drive circuitry is virtually identical to that discussed by Fremerey and Boden,² and used in the present commercial units. We focus our discussion on the signal processing and data-transfer circuitry which are different in the PC-based SRG controller.

A. The signal amplifier circuit

One of the critical factors in the amplifier design is the noise density of the first two stages of amplification. In a properly designed SRG controller, the thermal noise of the pickup coils should represent the limiting noise factor for inductively sensed timing signals. The pickup coils have a dc resistance of the order of 200 Ω , which has an equivalent Johnson noise density of about 2 nV/Hz^{1/2}. This noise figure, 2 nV/Hz^{1/2}, represents the upper limit restriction on the noise figure of the first-stage amplifier. In today's commercial SRG controllers, the pickup signal is inductively coupled into the amplifier circuit using a well-shielded 30:1 audio-range step-up transformer. This approach provides modest gain with a low noise figure. Our approach is to use low-noise operational amplifiers with a noise density of <2 nV/Hz^{1/2} at 400 Hz (see Fig. 2). These low-noise operational amplifiers were utilized in the first two stages of amplification with a net gain of about 75 dB.

After the initial amplification, the signal passes through a two-stage stagger-tuned Delyiannis-Friend (or multiple feedback) band-pass filter.⁷ The center frequencies of the two stages are at 375 and 675 Hz, respectively, both stages have a Q value of about 2.12, and there is an overall gain of about 28 dB from both stages. We have tried several band-pass filter designs with roughly equivalent results for filters which are not too narrow in bandwidth (<50–100 Hz or so) or too broad in bandwidth (>1–2 kHz or so). This filter design is similar to the design used in the commercial SRG controllers.

After band-pass filtering, the signal is amplified by a comparator circuit with a gain greater than 100 dB, and a pullup or Schmitt trigger is used to square off the signals. The output signal from the amplifier section is then a square wave with sharp zero-crossing transitions from which the zero-crossing timing is obtained.

B. The counter circuit

The counter circuit determines the rotor period by counting reference clock pulses between successive rotor signal zero crossings. The reference oscillator must have good short-term frequency stability, and a frequency that is high enough to avoid significant clock quantization effects, but not so high as to unnecessarily complicate the data transfer problem discussed in Sec. IV C. Temperature-compensated

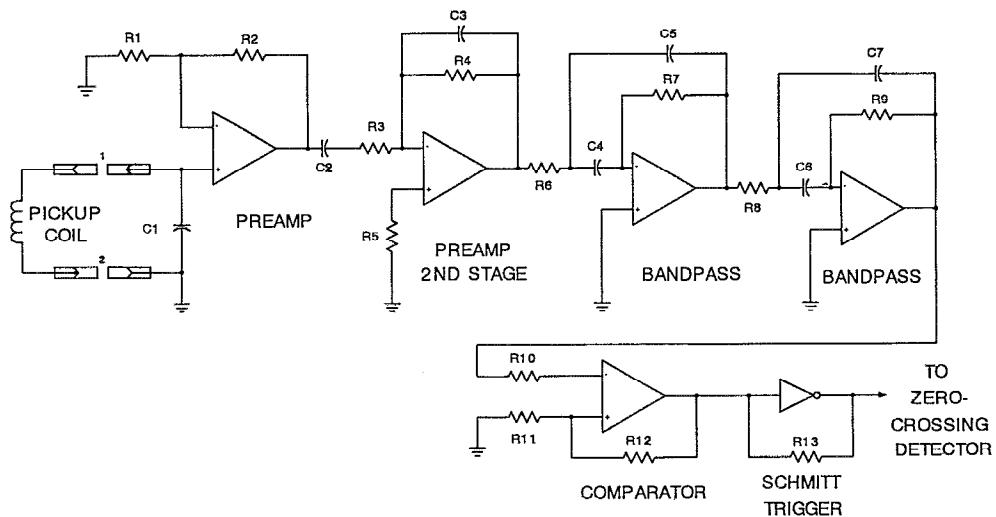


FIG. 2. Electrical schematic for the signal amplifier circuit.

quartz crystal oscillators were selected as offering the best frequency stability for a reasonable cost. A 10 MHz reference frequency was selected since it will effectively eliminate clock quantization errors, and the 40 000 counts accumulated during a rotor period at the lowest operating frequency, 250 Hz, can be accommodated by a 16-bit data transfer.

A short pulse is generated at each zero crossings by a zero-crossing detector (see Fig. 3), which consists of an exclusive-or gate; the same signal is applied to both inputs, but one of the inputs includes an RC delay. The RC delay is simply an in-series 100 k Ω resistor (R2) and a 100 pF ca-

pacitor (C1) shunted to ground. When the signal voltage passes through zero, the output of the exclusive-or gate is a 0.5 μ s duration pulse. This pulse triggers a pulse generator which produces a two-clock cycle (0.2 μ s) pulse, synchronized with the reference clock.

The output of the counter is connected to data latches (tristate buffers), which, in turn, are connected to the 16 data lines of the PC interface bus. When the timing signal voltage passes through zero, the output from the pulse generator enables the counter data latches for output to the PC bus, and enables the data-ready flag. The synchronization of the pulse

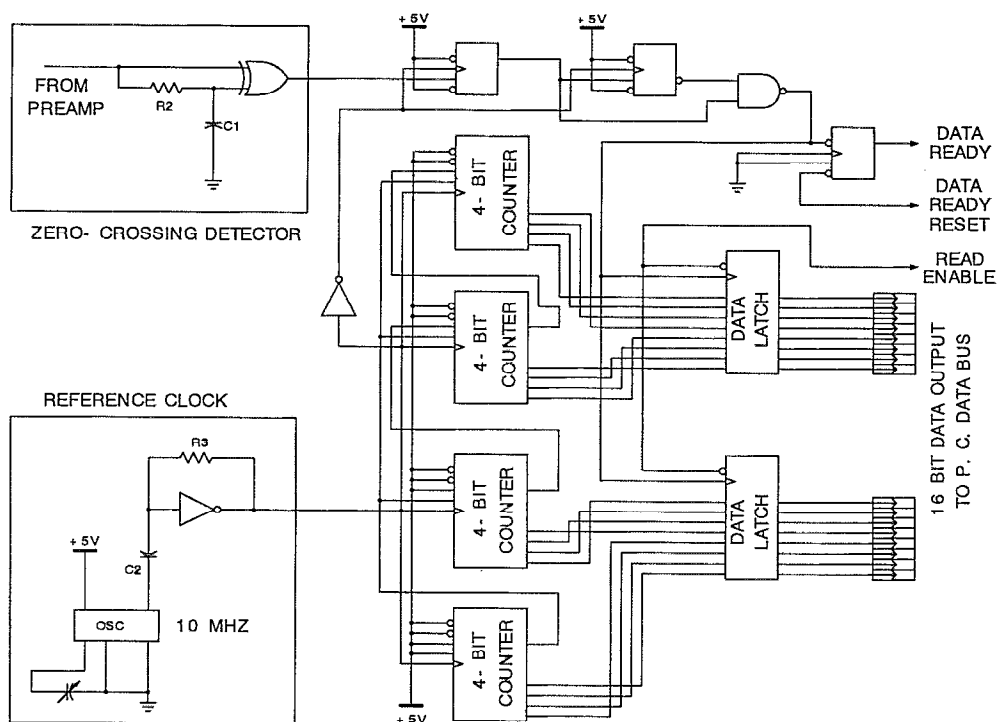


FIG. 3. Electrical schematic for the counter circuit.

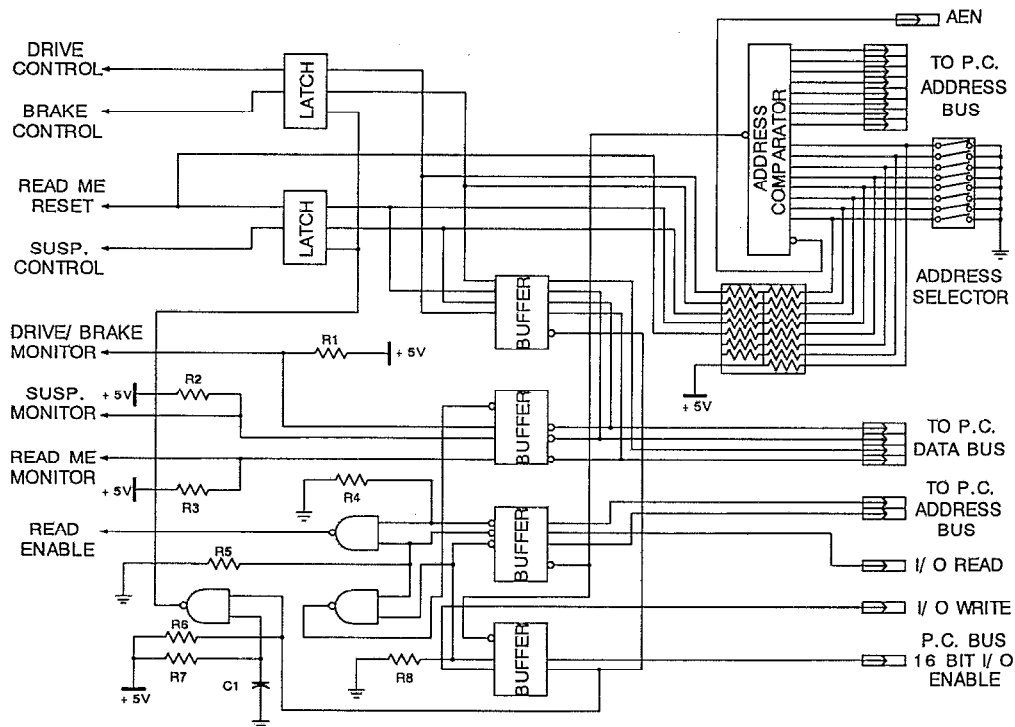


FIG. 4. Electrical schematic for the computer interface circuit.

generator output with the reference clock ensures that the value of the clock is not changing when the data latches are frozen. When the data-ready flag is raised, the computer program recognizes the data-ready condition, reads the current clock count and unfreezes the data latches. During the time the data flag is raised and the computer responds, the counters continue to accumulate clock counts so there is no loss of information and all zero crossings can be used in the computation of the deceleration rate and frequency.

The counter circuits were originally designed around the use of an 8-bit data transfer scheme [using the 8-bit I/O slots on the PC bus backplane (see Sec. IV B, below)] and thus 8-bit data latches and 4-bit counters were used so that the 16-bit information could be multiplexed. The current version of the interface circuit is designed around the use of 16-bit data transfer (using the 16-bit I/O slots available on the PC backplane), and the counter circuits could be simplified.

C. The computer interface

The use of PC software to maintain a cumulative time base and perform the sums required by the algorithms requires rapid data transfer between the peripheral card and the computer—the 16-bit contents of the on-board counter must be transferred to the PC, the data latches cleared, and the sums processed within one rotation period. Operating multiple boards further complicates the data transfer—the boards must be sequentially polled for “data ready” and the data transfer and processing accomplished for each board within a rotation period. We have taken two different approaches to the data transfer, each with their own advantages and disad-

vantages. Both techniques also execute the relatively simple task of controlling and monitoring board functions; suspension, drive, and brake.

The first interface design is based on the standard 8255 A CMOS programmable peripheral interface chip, which is utilized in many low-cost parallel I/O boards. This interface design has the advantage that it is reasonably straightforward to implement as the 8255 A is an industry standard peripheral interface chip, which is widely available. A single 8255 A has three 8-bit ports, two of which were used for the 16-bit data transfer and one was used for control and monitor logic (suspension monitor, brake, drive, data ready, first byte read enable, second byte read enable). The only limitation with the 8255 A was the fact that only 8-bit data transfers are possible and, thus, the 16-bit clock data from the counter circuits had to be broken into two 8-bit bytes, multiplexed, and the two bytes subsequently recombined in software. With this interface, we found that we could run and collect data from two SRG controller boards within a 386, 33 MHz PC.

In an attempt to increase the throughput of the PC-SRG interface, we also designed a 16-bit data interface, which resulted in an increase of slightly less than a factor of 2 in the maximum rate at which data could be processed. The only disadvantage to this design is the increase in complexity in the circuit design and implementation.

The 16-bit I/O circuit design is diagrammed in Fig. 4. This circuit consists of an address decoder segment and logic decoding circuitry to set the proper data latches for reading and writing capabilities. This interface design utilizes three sequential address values, each address having either 8 or 16

bits of associated information. The base address of the board is user selectable via an on-board DIP switch. An address comparator compares the 8-pin DIP switch setting with the 8 most significant bits of the 10-bit address byte from the AT interface bus. When the 8-bit DIP setting and the eight most significant address lines agree, i.e., the board is being addressed, the comparator issues a positive response via the AEN line of the interface bus, which tells the operating system that this is a valid address. We also use the AEN line, I/O read, I/O write, and the two least significant address bits as logic data to set the appropriate latches for data transfer to or from the PC bus.

The base address is used to write the control signals, e.g., turn drive motor on. The next address is used to read the monitor signals, data ready, ball suspension monitor, etc. The last address (base+10 binary) are used to transfer the 16-bit clock data.

Within the PC, 16-bit data transfers require the use of the 16-bit data-enable line to notify the operating system that 16 bits of data is to be transferred. When the SRG controller board has raised the data-ready flag and the condition is recognized by the control program, the SRG board is addressed by the control program to read from the base address+10 binary. The SRG board responds by enabling the AEN and 16-bit data-enable line, and by latching the current clock count onto the PC interface bus. Upon completing the data-read operation, the control program clears the data-ready flag by writing to the base address the appropriate logic value.

D. Other considerations

Connections to the SRG suspension head were made via connectors mounted on the PC peripheral board angle bracket. A miniature connector also was placed on the PC peripheral board angle bracket to monitor the rotor's signal strength and waveform from the second stage of the amplifier. This signal proves to be invaluable in troubleshooting SRG operational problems.

The circuits used in this controller for suspension, stabilization and brake/drive are essentially the same as those in the current SRG controllers, with one notable exception. Within the suspension circuit we have made provision for a small adjustable dc voltage bias to be applied to the suspension amplifier. This effectively shifts the vertical position of the magnetic suspension equilibrium position, i.e., it allows the location of the suspended ball to be moved up and down relative to the suspension head magnets. In theory there should be no need for this adjustment; however, variations in the magnetic field strength of the suspension's permanent magnets, the pole-face thickness, or the distance between the permanent magnets and the pole-face material result in changes in the magnetic center of the suspension head large enough to render some suspension heads unusable without the bias adjustment.

The ± 12 and ± 5 V dc power and ground for the SRG-PC circuits are taken from the PC power supply rails on the I/O edge connector. With all circuits operational (including the drive/brake circuit), the SRG requires about 220 mA of current at ± 12 V dc, and 200 mA at +5 V dc, and 10 mA at -5 V dc. Power supplies in most PCs have the capac-

ity to operate several SRG boards simultaneously, but are primarily limited by the +12 V supply. Attention also needs to be paid to the quality of all supply voltages; the voltage and ground supply lines to the signal processing circuits are particularly important. Noise present on the dc power rails and problems arising from poor ground will introduce noise in the signal processing circuits which will limit the performance of the SRG by producing false zero crossings. Simple capacitive filtering of the power supply lines is generally adequate to eliminate this problem.

E. Control program

The ability to read 16-bit data from individual memory locations, the ability to monitor parity changes in the monitor byte, the overall execution speed, and the ease in implementation of the control logic are important considerations in the development of a control program. Control of the PC-SRG board was accomplished using a Pascal-based program running under DOS. As noted before, with different types of computers we have simultaneously operated multiple controller cards—up to four with a 33 MHz 80486-based PC. An obvious concern with simultaneous operation is errors associated with the failure to detect data-ready conditions and read the associated data on multiple boards before any of the next zero crossings occur. We have never observed such errors and have more than enough operating time to indicate that this is not a problem for normal operating conditions.

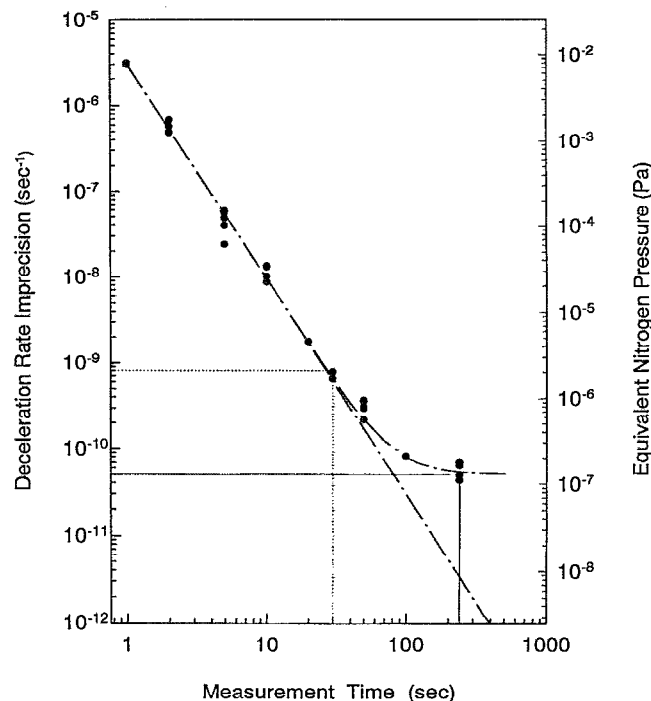


FIG. 5. Imprecision of rotor deceleration rates as a function of measurement time. Each point is the standard deviation about the mean of a number (10–100) of sequential deceleration measurements. Included are data obtained over a period of several days. The dashed line illustrates the predicted dependence on the five-halves power of the measurement time. The horizontal lines indicate the imprecision for 30 s (dotted) and 240 s (solid) measurement times.

V. PERFORMANCE

During the development of the PC-based SRG controller, numerous tests were conducted to verify the accuracy of the results obtained with the present controller design. As an elementary check for hardware and programming errors, pickup signals were simultaneously processed by both PC-based and commercial controllers; for measurement times of less than 30 s the results were identical. Similarly, the frequencies of low-noise signals were determined with both the PC-based controller and with high-accuracy conventional frequency counters; the results agreed to within 1 part in 10^6 , which is within the uncertainty of the controller's reference oscillator.

More telling are the results in Fig. 5, where the imprecision in the measured deceleration rate (DCR) of an Invar (low thermal expansion nickel-iron alloy) ball is graphed as a function of the measurement time t . The imprecision, or standard deviation about the mean value, was calculated from several (10–100, depending on the measurement time) successive measurements of the deceleration rate. As can be seen, the uncertainty in the measurement does decrease as $t^{-5/2}$ for measurement times up to about 100 s, in agreement with the predictions of Eqs. (13) and (14). For longer times the imprecision asymptotically approaches a value of 5×10^{-11} DCR, indicating that the measurements are limited by factors other than the phase noise in the pickup signal. Several factors can contribute to the long-time limit, including instabilities of the rotor's magnetic moment(s), rotor temperature, and reference (clock) oscillator frequency. We have also used a temperature-controlled reference oscillator in place of the on-board temperature-compensated oscillator. This resulted in a factor of 2 improvement in the limiting imprecision, so at least part of the limit is due to reference oscillator instability.

Calculations using all zero crossing returned the same logarithmic time derivative as obtained when using only every other zero crossing, but with an imprecision reduced by $\sqrt{2}$, as predicted in Sec. III.

The band-pass filter in the signal-processing electronics, and the declining strength of the inductive pickup signal, limits SRG operation to a lower-frequency limit of about 350 Hz. However, at higher frequencies the increase in pickup signal strength compensates for the high-frequency rolloff of the filter, and we have successfully operated at frequencies up to 1500 Hz. In general, results obtained at different frequencies are again consistent with the predictions of Eq. (14). We have already found operation over an extended frequency range, without interference from the automatic frequency control of the commercial controllers, to be useful for several different applications.

Finally, by comparing the imprecision of deceleration rate measurements for 30 and 240 s measurement times (indicated in Fig. 5 by the dotted and solid lines, respectively) we note that there is a 20-fold improvement over the limit obtained with the present commercial gage controllers. This implies that the low-pressure resolution of the SRG can be significantly improved by the use of the longer sampling times afforded with the present design.

ACKNOWLEDGEMENT

The authors would like to thank Steve Parks for assistance in the design of the zero-crossing detector, counter, and 8-bit I/O interface circuitry.

¹J. W. Beams, D. M. Spitzer, Jr., and J. P. Wade, Jr., *Rev. Sci. Instrum.* **33**, 151 (1962).

²J. K. Fremerey and K. Boden, *J. Phys. E* **11**, 106 (1978).

³S. Dittmann, B. E. Lindenau, and C. R. Tilford, *J. Vac. Sci. Technol. A* **7**, 3356 (1989).

⁴J. Setina and J. P. Looney, *Vacuum* **44**, 577 (1993).

⁵J. J. Snyder, *Proceeding of the 35th Ann. Frequency Control Symposium*, USAERADCOM, Ft. Monmouth, NJ, May 1981.

⁶J. K. Fremerey, *J. Vac. Sci. Technol. A* **3**, 1715 (1985).

⁷M. E. Van Valkenburg, *Analog Filter Design*, 1st ed. (Holt, Rinehart, and Winston, New York, 1982).